QUASI-OPTICAL ANTENNA ARRAY AMPLIFIERS

Jon Schoenberg, Tom Mader, Boyd Shaw, Zoya Basta Popović

Department of Electrical and Computer Engineering
University of Colorado, Boulder, CO 80309

Abstract -- **Several quasi-optical transmission wave amplifiers are presented: (1) a two-level power-combining PHEMT patch-antenna lens amplifier with 8 dB of absolute power gain at 9.7 GHz used for beamforming and beam-switching; (2) a saturated class-A polarization-preserving 24-MESFET patch array which produces 0.7 Watts at 10 GHz with 21 % power-added efficiency; and (3) an X-band 2-stage low-noise CPW PHEMT amplifier cell using anti-resonant slot antennas with 21.7 dB active gain, 3.2 dB noise figure and a 6 % 3-dB bandwidth.**

Summary

Quasi-optical amplifiers demonstrated to date are grid [1] and antenna array [2-6] amplifiers. These devices receive, amplify, and re-radiate a wave in transmission. In [6], the amplifier is designed to be a discrete lens -- the array is fed from a focal point in the near field, and only a small portion of the feed power is diffracted. This lens amplifier exhibited 5.7 dB of power gain at 10.25 GHz when fed from a focal point. A 28-PHEMT grid oscillator was designed specifically as a feed for the amplifier, and beam-steering was demonstrated in both E and H planes as the grid oscillator was moved along the focal arcs of the lens [6].

Here we present beamforming and beam-switching results with a dual grid-oscillator feed, as shown in Fig.1. When both grids are on, the output radiated pattern of the linear lens amplifier is a superposition of the patterns for the two individual feeds, which makes beamforming possible. Fig.2 shows examples of measured dual-beam patterns in the E and H planes of the lens. In the E-plane, the two grids were placed at 0° and 24° along the focal
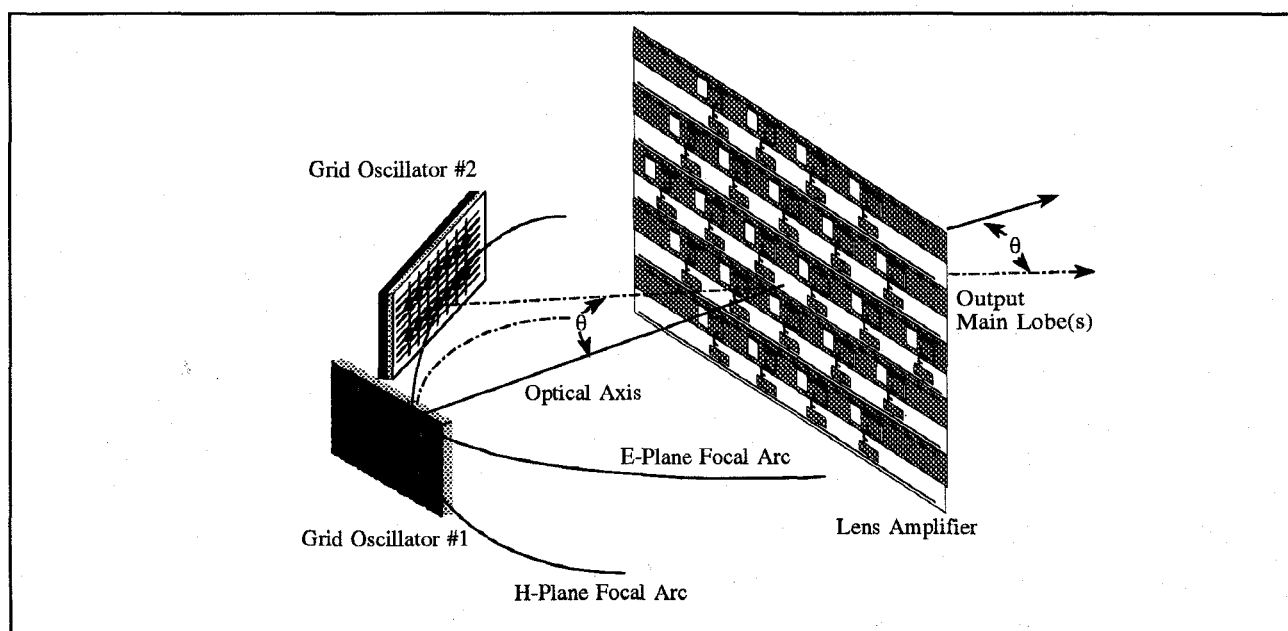

Figure 1: A patch antenna lens amplifier with a dual grid-oscillator focal point feed. The shaded patches, microstrip circuits, and ground planes are on the backside of the array.

arc (the resolution of our rotation stage is 3°) and the amplifier pattern, shown in solid line, shows equal-power beams at 0° and 24°. Two beams at 21° in the H-plane are shown in dashed line in Fig.2. The individual grid oscillators can also be bias-switched one at a time, and so the amplifier pattern can be switched between a finite number of beams at different angles. In this case, the switching speed is limited by the oscillator settling time. By keeping the oscillators biased at the threshold of oscillation and pulsing the gate bias, a switching frequency of 5 kHz was measured (0.2 msec switching rate). It was verified that the grid oscillator that is off does not affect the pattern of the lens.

As the input power to the lens amplifier is increased, the center elements start saturating. This makes the saturation curve of the array more linear than that of a single element. However, when the lens is nonuniformly saturated, its radiation pattern changes: the main lobe broadens and the sidelobes are reduced. Fig.3a shows the measured gain compression curve of the lens using a 1-W TWT amplifier at the output port of a HP71500A Transition Analyzer. Fig.3b shows the pattern broadening corresponding to the 3-dB compression point of the ERP.

The noise figure of the lens amplifier was measured using a Noise Com 3208A noise source with an ENR of 29 dB, a HP8593E Spectrum Analyzer and a 38-dB preamplifier. A Y-factor measurement yields a noise figure of 3.45 dB at 9.75 GHz with a corresponding gain of 8 dB, as shown in Fig.4. The amplifier described in [6] exhibited two peaks in the gain frequency response (at 10.25 and 9.7 GHz) due to mismatched resonant

frequencies of the patches across the array. The antennas were matched by eliminating effects of ground planes close to radiating edges of a few of the patches in the array. This improves the gain to 8 dB at 9.75 GHz.

The lens presented above was designed for maximum gain. A low-noise amplifier is designed to receive a plane wave and focus it down to a focal point at which a mixer can be placed. A single cell of the low-noise amplifier is shown in Fig.5a. The input antenna is an anti-resonant folded-slot loaded with a resistor and capacitor, which act as part of the stabilization network. The output antenna is an anti-resonant off-center fed slot with an input impedance of 100 Ω. The measured 2:1 VSWR bandwidth is 25% at the 10-GHz second

(A)

(B)

Figure 3: (a) Measured gain compression of the lens amplifier effective radiated power (ERP). (b) Radiation pattern corresponding to the amplifier operation in the linear regime (dashed line), and 3-dB into compression (solid line).
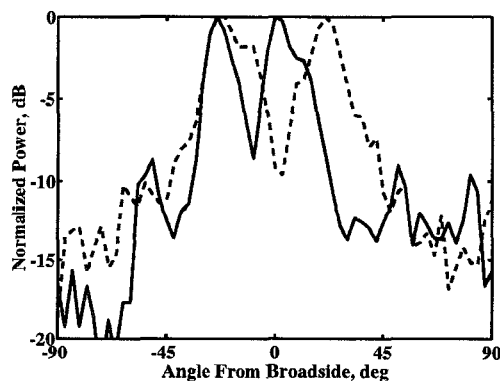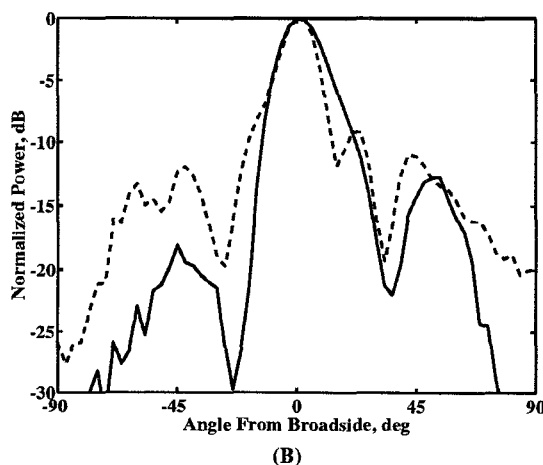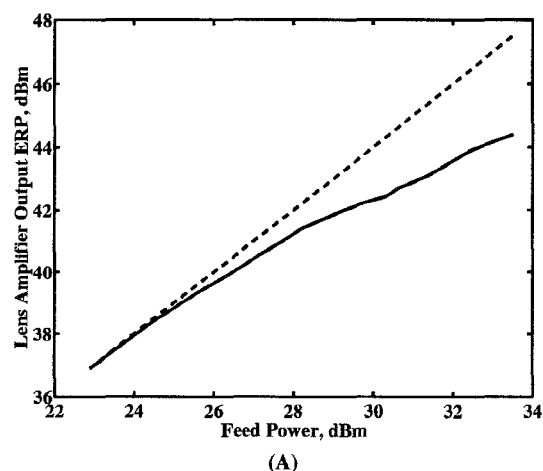
Figure 2: Measured normalized beamforming lens amplifier radiation patterns for two different positions of the grid oscillator feeds in E- and H-planes (solid and dashed lines, respectively).

resonance. The slots were designed using an approximate full-wave method described in detail in [7]. The amplifier was fabricated on a $\varepsilon_r = 2.17$, 0.79-mm thick substrate with Avantek ATF 35376 PHEMTs. A passive unit cell with a CPW through line in place of the amplifier was measured for calibrating the slot antenna pair frequency response. The measurements show that the 2-stage amplifier in the single element contributes 21.7 dB at 9.7 GHz, with a free-space-measured noise figure of 3.2 dB. A polarizer at the input improves the through-gain by 1.4 dB. The noise figure of the entire array should be the same as that of the single element.

Most of the amplifiers demonstrated to date use orthogonal polarization for input and output waves as a means of isolation. The alternating ground planes in the lens amplifier allow for arbitrary polarization, as was demonstrated earlier on a polarization-preserving amplifier and a linear-to-circular amplifier in [2]. The polarization-preserving 24-MESFET patch array described in [2] was designed for maximum gain at a lower bias point (20 mA, 2 V) per device. The s-parameters at a higher bias point (40 mA, 4 V) are practically identical, except for an increase in $|S_{21}|$. Since, to a first approximation, only this parameter changes (decreases) when a MESFET is saturated, the design for a saturated class-A amplifier at the high bias point should be the same as the low-bias point linear design. The array is built on a $\varepsilon_r = 2.17$, 0.5-mm Duroid substrate with Avantek low-cost general purpose ATF 13484 MESFETs.

First a single amplifier unit cell was measured between two polarization-aligned 16-dB gain horn antennas, placed in its far field. The horns were connected to a 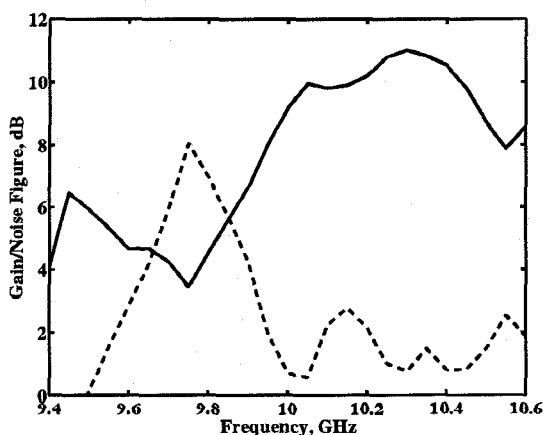HP71500A Transition Analyzer, used to measure the power saturation curves for several bias points, shown in Fig.6. Then the entire array was measured in the same manner. A 10-W TWT-fed horn provided a total input power to the array of 64 mW (2.7 mW/device) in the far field. With a constant input power and a total array drain current of 1 A, the output power was measured for several drain-bias voltage points, and the results are given in Table 1. For obtaining the values in Table 1, a patch gain of 5 dB was used.

The source power is insufficient to saturate the array at the high bias points since the feed horn is in the far field. This can be seen in Fig.6, where the power per element in the array is plotted along with the saturation curves for a single element. The average power per element in the array is 1-2 dB lower than that of a single element tested alone, which means that the array combining is lower than in a uniform array. For this low-cost class-A amplifier, an output power of 0.7 W with 21 % power-added efficiency was measured at 10 GHz for an input power of $P_{DC} = 3$ W.
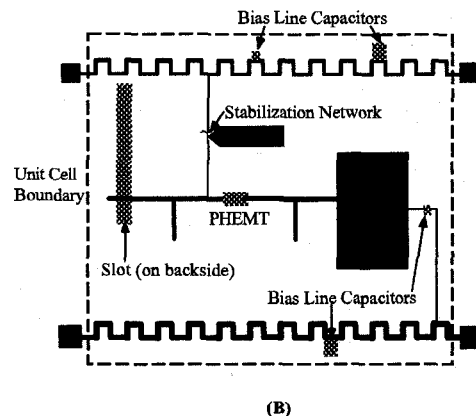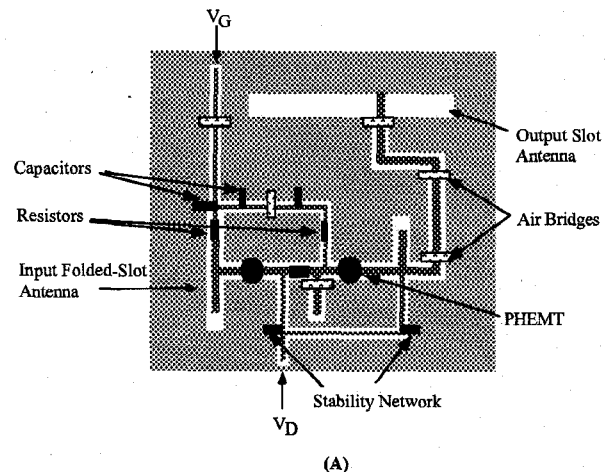

(A)

Figure 4: Measured gain (dashed line) and noise figure (solid line) of the lens amplifier.

(B)

Figure 5: (a) Single element of an X-band low-noise amplifier array. (b) Single element of a V-band patch-slot amplifier design.
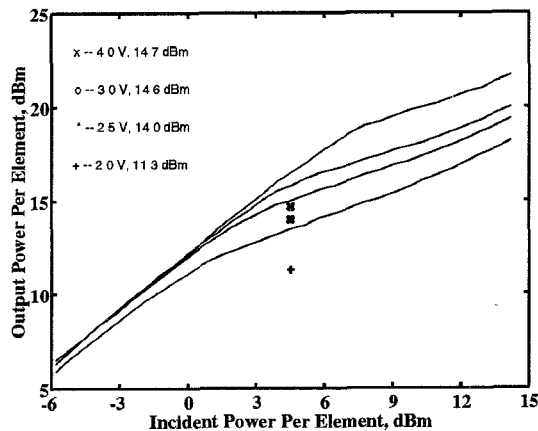
Figure 6: Saturation curves of a single-element free-space amplifier for a constant drain current and several drain bias voltages. The superimposed symbols represent measured array power levels, divided by the number of elements $(N = 24)$.

The presented amplifiers use microstrip circuits with patch antennas, or CPW circuits with slot antennas. An example of a different amplifier with slots on the receiving side of the substrate, and microstrip amplifiers and patches on the transmitting side, is shown in Fig. 5b. It was designed to operate at 60 GHz with 7 dB gain. Sixteen and 36-PHEMT monolithic arrays were fabricated by the Martin Marietta Research Labs in Baltimore and will be tested in the near future. DC tests indicate good yields across the wafers.

Acknowledgements

References

[1] M. Kim, E. A. Sovero, J. B. Hacker, M. P. De Lisio, J.-C. Chiao, S.-J. Li, D. R. Gagnon, J. J. Rosenberg, D. B. Rutledge, "A 100-element HBT grid amplifier, " *IEEE Trans. on Microwave Theory and Techniques, Vol. MTT-41, No.10,* pp.1762-1771, Oct 1993.

[2] T. Mader, J. Schoenberg, L. Harmon, Z. B. Popović, "Planar MESFET Transmission Wave Amplifier," *IEE Electronic Letters, Vol. 28, No. 19,* pp. 1699--1701, September 1993.

[3] N. Sheth, T. Ivanov, A. Balasudramaniyan, A. Mortazawi, "A 9-HEMT spatial amplifier," *IEEE MTT International Symposium Digest,* pp. 1239--1242, San Diego, May 1994.

[4] J. S. H. Schoenberg, Z. B. Popović, "Planar lens amplifier," *IEEE MTT International Symposium Digest,* pp. 429--432, San Diego, May 1994.

[5] T. P. Budka, M. W. Trippe, S. Weinreb, G. M. Rebeiz, "A 75 GHz to 10 GHz quasi-optical amplifier," *IEEE Trans. on Microwave Theory and Techniques, Vol. MTT-42, No.5,* pp.899--900, May 1994.

[6] J. S. H. Schoenberg, S. C. Bundy, and Z. B. Popović, "Two-level power combining using a lens amplifier," *IEEE Transactions on Microwave Theory and Techniques, Vol. MTT-42, No. 12,* pp. 2480-2486, December 1994.

[7] B. D. Popović, *CAD of Wire Antennas and Related Radiating Structures,* Research Studies Press, Ltd. (John Wiley & Sons, Inc.), Chichester -- New York, 1991.

$V_{DC}(V)$ for $I_{Dtot} = 1$ A	Gain (dB)	Output Power (W)	Drain Efficiency (%)	Power-Added Efficiency (%)
2.0 V	8.6	0.3	16	13
2.5 V	9.7	0.6	24	22
3.0 V	10.3	0.7	23	21
4.0 V	10.4	0.7	18	16

Table 1. Measured gain, power and efficiency of the 24-MESFET array at 10 GHz for an input power of 64 mW (2.7 mW/device) and a constant total drain current of 1 A.